Journal of Environmental Radioactivity 237 (2021) 106668

Contents lists available at ScienceDirect

Journal of Environmental Radioactivity

journal homepage: www.elsevier.com/locate/jenvrad

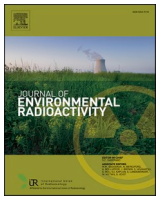

Rare earth elements in uranium ore deposits from Namibia: A nuclear forensics tool

Dakalo Madzunya [a,*], Vera Uushona [b], Manny Mathuthu [a], Wanke Heike [c]

[a] Center for Applied Radiation Science and Technology (CARST), North-West University (Mafikeng), Cnr Albert Luthuli Road and University Drive, 2735, Mmabatho, South Africa
[b] National Radiation Protection Authority, Ministry of Health and Social Services, Windhoek, Namibia
[c] Department of Geography and Environmental Management, University of the West of England, UK

ARTICLE INFO

Keywords:
Rare earth elements
Nuclear forensic signatures
Uranium ore
ICP-MS
PCA

ABSTRACT

Rare earth elements (REE) concentrations and pattern remains largely unchanged during the process of milling and can thus provide strong evidence of the origin of the material. The aim of this study was to determine the rare earth elements in uranium ore deposits as a nuclear forensics tool. Uranium ore from three mines were collected and analyzed using an inductively coupled plasma mass spectrometry (ICP-MS) to determine the concentrations of rare earth elements. A non-parametric Kruskal-Wallis test and a *pair* wise comparison test was used to test for significant difference in the concentration of REEs between the mines followed by principal component analysis (PCA). The REE concentration were normalized with C1-Chondrite values to determine the REE pattern. The total concentration of the REE ranged from 131.38 to 161.77 ppb, 266.27 to 840.37 ppb, 177.86 to231.51 for Mine 1, 2 and 3, respectively. The mean ∑REE obtained was in the order M2>M3>M1. The pairwise comparison test of the pair M1 and M2 was found to be less than 0.05, indicating a significant difference in the samples. The REE pattern is mostly similar for all the ore samples with pronounce Eu anomaly, enriched LREE and depleted flat HREE. The PCA results indicates that the ore samples can be distinguished from each other.

1. Introduction

In the early 1990 incidents of illegal possession, transfer and unauthorized acts involving nuclear material were reported mainly from Europe due to the breakup of the Soviet Union (IAEA, 2015). From these incidents the need in international communities arose to scientifically characterize the nuclear and other radioactive materials found outside of regulatory control, to determine its processing history, origin and potential illicit trafficking route (Keegan et al., 2016) giving rise to the discipline nuclear forensics.

Nuclear forensics is a science that contributes to criminal investigations of interdicted nuclear materials such as uranium, plutonium and other radioactive material to determine the origin or intended use of the material (IAEA, 2002). This is provided by identifying any characteristics or group of features that may be significantly used to assist in distinguishing materials from one another or to determine the origin of material processes known as nuclear forensics (Hutcheon et al., 2015).

Uranium ore is the main raw material in the front end of the nuclear fuel cycle in the production of nuclear energy. It is formed in a wide range of geological settings, including deep magmatic to surficial conditions, and range in age from archaeon to recent with uraninite being the most and abundant component of uranium ores (Mercadier et al., 2011). Nuclear forensics scientists have characterized uranium ore and nuclear materials in terms of isotopic composition, chemical impurities, the age, the morphology, trace element and rare earth elements as nuclear forensics signature (Mayer et al., 2011). Each nuclear sample carries signature of the materials from which it was made or the process to which it was subjected. Such signatures may be related to chemical processes, such as extraction, ion exchange, precipitation, or may be due to physical processes.

Rare earth elements (REE) are a group of 17 elements that frequently present together in varieties of igneous rocks at different concentrations (Rosa and Sarkis, 2011) and are efficient in providing evidence of the origin and genetic type of the uranium ore. This is largely owed to its

* Corresponding author.
E-mail addresses: dmazunya@nmisa.org (D. Madzunya), Vera.Uushona@mhss.gov.na (V. Uushona), manny.mathuthu@nwu.ac.za (M. Mathuthu), heike.wanke@yahoo.de (W. Heike).

https://doi.org/10.1016/j.jenvrad.2021.106668
Received 9 September 2020; Received in revised form 23 April 2021; Accepted 19 May 2021
Available online 8 June 2021

distinct pattern different for the kind of deposit and remains largely unchanged under various processing conditions (Mercadier et al., 2011; Keegan et al., 2014; Balboni et al., 2017). These REE are the 15 lanthanides La, Ce, Pr, Nd, Pm, Sm, Eu, Gd, Tb, Dy, Ho, Er, Tm, and Lu with atomic numbers ranging from 57 (lanthanum) to 71 (lutetium) and scandium and yttrium. Amongst the 15 lanthanides, 14 elements occur in nature except for promethium with atomic number 61 (Kanyan, 2015). REE can be divided into two categories, Light REE (LREE) (La-Gd) and Heavy REE (HREE) (Tb-Lu). LREE can be fractionated from HREE throughout the formation of minerals like apatite, garnet, monazite, sphene and zircon (Reading, 2016).

Nuclear forensics scientists have employed REE as a possible nuclear forensics signature (Balboni et al., 2017; Bradley et al., 2020; Frimmel et al., 2014; Khumalo and Mathuthu, 2018; Spano et al., 2017). Khumalo and Mathuthu (2018) investigated REE in uranium ore samples from South Africa using inductively coupled plasma mass spectrometry. The REE fingerprint that the authors obtained suggested that the uranium was embedded in uraninite, phosphorite deposit in apatite and fluorapatite minerals and they obtained a light REE uniformity and heavy REE fractionation with strong positive Tb anomaly in their study. The concentrations of REE in uranium ore can be used to distinguish between different ore deposit and thus form part of the nuclear forensic signature of the different uranium ore deposits (Frimmel et al., 2014; Spano et al., 2017). The fractionation and relative enrichment or depletion of Ce or Eu together with the relative elemental REE concentration existing in a sample could act as a forensic tool in the identification of a possible geological setting of origin. For instance, if the REE signature showed no fractionation or anomaly, the sample would likely come from a deposit derived from synmetamorphic deposits or sandstone (Donard et al., 2015).

Namibia is a major exporter of uranium ore concentrate and produced a total of 40849 t of uranium during the period 2018 and 2019 (WNA, 2019). There is thus a need to develop nuclear forensic signatures in case of interdictions of nuclear material and thus REEs can be used as signatures. The data obtained from these REE can be used as nuclear fingerprint for source attribution and contribute to the National Nuclear Forensics Library (LaMount et al., 2011; IAEA, 2018a).

2. Materials and method

2.1. Study area

The Erongo region located in the central western part of Namibia is rich in uranium mineralization's and the hub of Namibia's uranium mining. There are currently two uranium mines in operation, two under care and maintenance and five active exploration companies (NUA, 2019).

The uranium mineralization is concentrated in the Central Zone of the Pan-African Damara Orogen (Fig. 1). The Central Zone of the Pan-African Damara Orogen is an intracontinental zone with a stretch of 400 km between the Congo and Kalahari cratons (Basson and Greenway, 2004). The Damara Belt hosts hard rock uranium deposits of the Mesoproterozoic Damara Supergroup (Miller, 2008).

The region (Fig. 2A) consists of primary intrusive uranium deposit that is associated with bodies of alaskite, granite, pegmatite and monzanite and surficial paleogene to recent near-surface sediments or soils containing uranium from intense weathering and erosion of granites known as calcrete secondary deposit that formed in paleo-valleys of ancient rivers (IAEA, 2009; MME, 2010; IAEA, 2018b; IAEA, 2020). The dominant uranium mineral in the alaskite is uraninite, whilst the dominant mineralization in the calcrete is carnonite (MME, 2010). Fig. 2 B shows the location of known uranium deposits in Namibia. Mines are referred to as M1, M2 & M3 due to confidentiality agreements.

2.2. Sample collection and preparation

A total of 25 crushed uranium ore samples were collected from the mines fine ore stock pile at the same time. This constituted of 8 samples from mine 1, 9 samples from mine 2 and 8 samples from mine 3. The samples were packaged in 0.50 kg polyethylene bags (Fig. 3) and transported to the Center of Applied Radiation Sciences (CARST), North-West University analytical laboratory for analysis.

About 0.5 g of each sample was digested in an acid mixture consisting of 9 mL of 37% of hydrochloric acid and 3 mL of 55% of nitric acid in standard 75 mL high pressure digestion vessels. The mixture was digested according to the manufacturers instruction at temperature 160 °C and total digestion time of 30 min (PerkinElmer, 2017). A control reagent blank (without sample) of the same mixture of nitric and hydrochloric acids have been digested at the same time. After digestion, each aliquot was transferred to a 50 mL sample bottle and diluted with deionized water. The solution was allowed to stand for 24 h before analysis. 3 mL of the prepared 50 mL solution was transferred to 10 mL ICP-MS analysis sample holder container.

2.3. Sample analysis

Samples analyses was performed with PerkinElmer ICP-MS NexION 2000C. The ICP-MS was preferred analytical technique due to its multi-element analysis capabilities and high sensitivity with detection limit of ppt-ppq (Bazilio and Weinrich, 2012). The NexION 2000 ICP-MS has

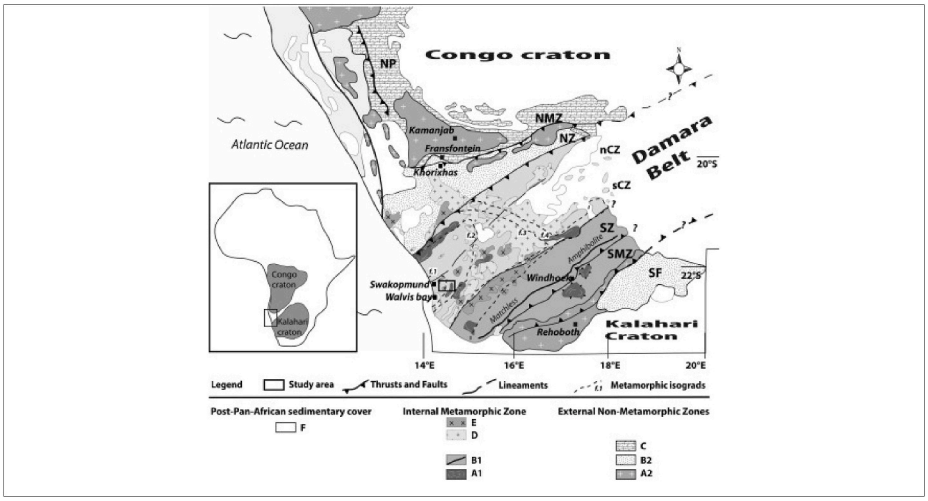

Fig. 1. Location of the Damara Orogenic belt between the Congo and Kalahari cratons (Toé et al., 2013).

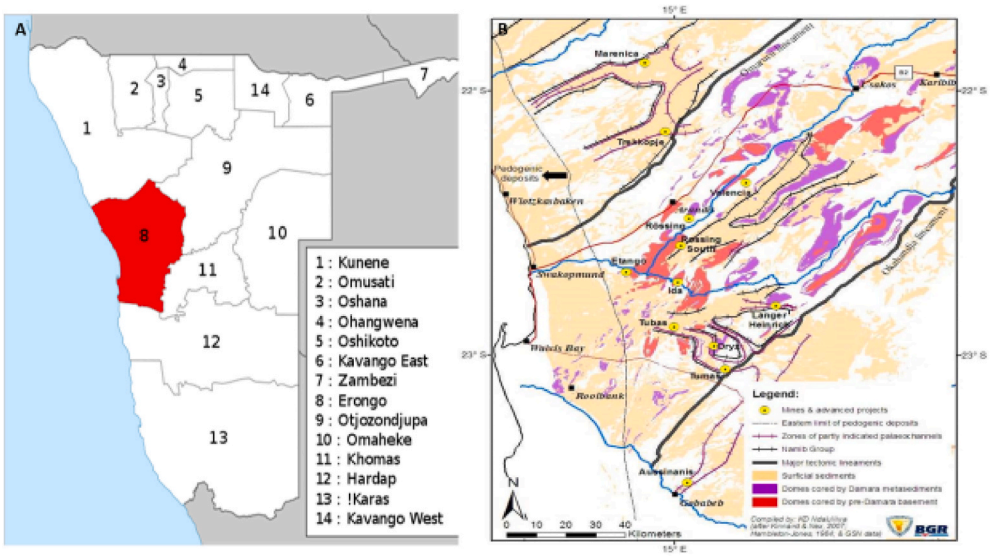

Fig. 2. Map A, showing Erongo region in red (MURD, 2020), Map B, Namibia's known uranium deposits (MME, 2010). (For interpretation of the references to colour in this figure legend, the reader is referred to the Web version of this article.)

Fig. 3. Examples of packaged sample.

Quadrupole ion deflector and dual mode detector (Fig. 4). The instrument was optimized using the automated SmartTune™ procedure prior to measurements. A 10 mg/L PerkinElmer multi element calibration standard was used as a reference material.

The samples were loaded on the auto sampler in the following sequence: a blank sample, standard and then the samples. The sequence of measurements is depicted in Fig. 5. The blanks and standard were for quality control checks and were run at every ten sample set of measurement (Keegan et al., 2008). Auto sampler sampling capillaries were rinsed with deionized water prior to analyses of each sample. The liquid sample is pumped into the nebulizer via sampling capillaries and converted into gaseous form. The gaseous droplets moved into the plasma torch and turned into ions. The ions were separated based on their mass-to-charge ratio by the mass separation component. The ions were then converted into an electrical signal by the ion detector, which was then quantified into elemental concentration using the Syngistix™ Nano application software. Elemental concentration was acquired with the total quant method. Molecular and Isobaric interference due to oxides and hydroxides were addresses as described in the article by Khumalo and Mathuthu (2018).

2.4. Data analysis

Statistical analyses were performed using Statistical Package for the Social Sciences (SPSS) v25 (IBM).Principal Component Analysis (PCA) was employed to identify trends and grouping (Keegan et al., 2008; Švedkauskaitė-LeGore et al., 2008; Reading et al., 2016) in R statistical software (Rstudio team, 2020). The data set consisted of 14 variables (REE) and 3 independent groups (the mines), non-parametric Kruskal--wallis test that allowed for comparison of more than two independent groups was used to test for significance difference ($p < 0.05$) in the concentration of REE between different mines. For REE determined to significantly differ a post–hoc pair wise comparison test was undertaken to determine which mines had significantly different REE concentrations. The scale of the pair wise test is 0–1, a $p < 0.05$ suggests significant difference and $p > 0.05$ suggests no significant differences. The abundance of the REE was normalized with the known C1-Chondrite values (Anders and Grevesse, 1989) and illustrated as graphs plotted in logarithmic scale. If the REE pattern is above the general trend then the anomaly is defined as positive and the anomaly is said to be negative if it is below the trend (Kanyan, 2015). The La_N/Yb_N was used to quantify LREE enrichment and HREE depletion and the ratio La_N/Sm_N and Gd_N/Yb_N was used to provide the degree of LREE and HREE fractionation respectively (Wang and Liang, 2015).

3. Results and discussions

The following are the results obtained after analyzing the uranium ore samples using an inductively coupled plasma mass spectrometry (ICP-MS).

3.1. Abundance of REE

The mean sum concentration of REE in the uranium ore deposit range as follow: 131.38–161.77 ppb, 266.27–840.370 ppb, 177.86–231.51 ppb for M1, M2 and M3 respectively. The mean of the concentration is of the order M2 >M3> M1, with M2 having the most

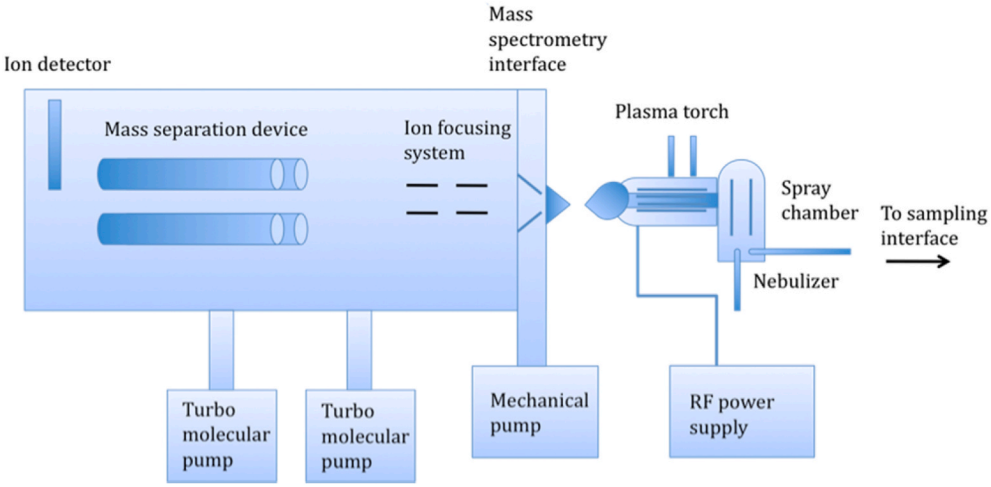

Fig. 4. The basic components of an ICP-MS system (Thomas, 2008).

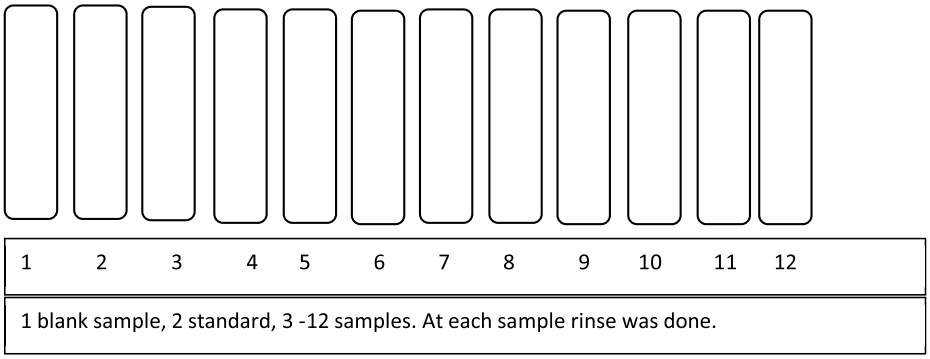

Fig. 5. ICP-MS sequence of measurements.

abundance of REE.

The uranium ore samples are dominant with LREE which accounts for more than 80% of the ∑REE in all the mines. M1 has the most abundance of LREE with 90% of the ∑REE. LREE dominant element is Ce with more than 40% of the ∑LREE and Dy is the dominant HREE with over 40% concentration of the ∑HREE in all mines.

The result of the concentrations of REE in uranium ore from the study can be used to distinguish between the different ore samples and thus form part of the nuclear forensic signature of the Namibia uranium ore deposits.

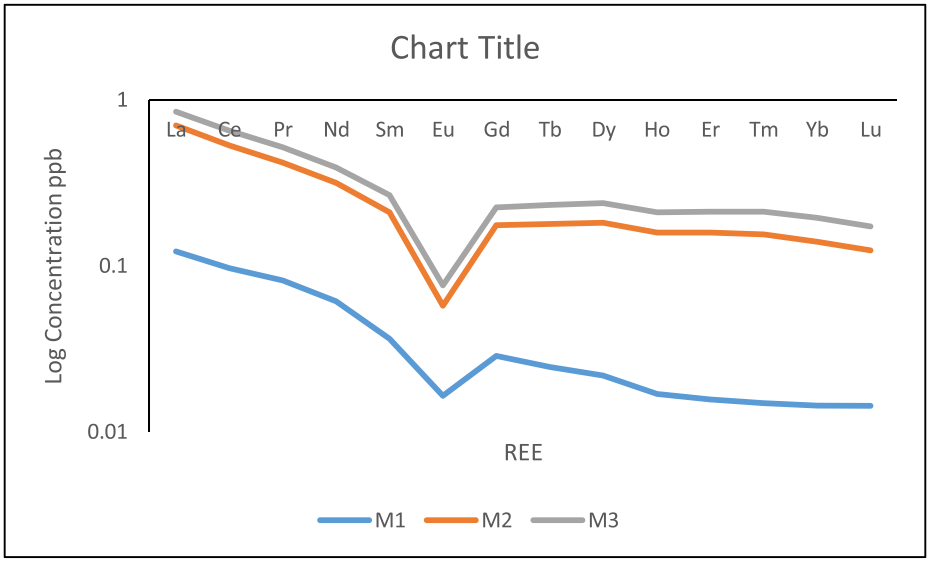

Fig. 6. C1-chondrite normalized REE patterns for uranium ore from Mines 1, 2 and 3.

3.2. Patterns of REE relative to C1-Chondrite

Fig. 6 below shows the REE C1-chondrite normalized patterns. The REE patterns were broadly similar for all the samples with a negative slope of LREE and relative flat HREE. This provides an indication of the consistency of geochemical distribution of REEs in the samples.

The negative slope of LREE is a characteristic of LREE enrichment and HREE depletion which is quantified with the ratio of La_N/Yb_N. When the ratio is greater than or equal to 1 then the samples are enrichment with LREE and depleted with HREE. The ratio La_N/Yb_N was 8.55 $_{M1}$, 4.62_{M2} and 2.67_{M3}, meaning all ore samples are enriched with LREE and depleted with HREE with M1 ore the most enrich with LREE. The degree LREE fractionation of La_N/Sm_N of 3.36_{M1}, 3.33_{M2} and 2.62_{M3} are slightly higher than that of the HREE fractionation, Gd_N/Yb_N of 1.98_{M1}, 1.1_{M2} and 0.90_{M3}. The LREEs have slightly larger ionic radii relative to the HREEs, and this may explain the higher enrichment for LREEs (Balboni et al., 2017).

The REE pattern is further characterized with a distinct negative Eu anomaly that implies a lower abundance of Eu compared to its neighboring REE. Similar REE pattern were observed for uranium ore from Luthi mine in Finland and Moore Lake mine in Australia with similar deposit from magmatic/intrusive environment (Mercadier et al., 2011; Spano et al., 2017), and CN patterns of rocks from the Damara Orogen of Namibia displayed an equally relative flat plot with strong negative Eu anomaly (Falster et al., 2018). A negative Eu anomaly is consistent with mineralization fluids associated with granitic hydrothermal melting or weathered granitic deposits (Varga et al., 2010) and in primarily sandstone hosted rollfront/calcrete uranium deposits found in Botswana (Ntsohi et al., 2020). The characteristic observed is similar to those of younger granites that are characterized by LREE-enrichment with La_n/Yb_n ranging between 5.28 and 13.46 with moderately fractionated LREE, flat heavy REE patterns and moderately to strongly negative Eu anomalies (Bahariya, 2018). Conversely, ore from different deposits such as breccia deposit of Olympic dam Mine (Australia) REE pattern displayed a positive Eu anomaly (Keegan et al., 2008) and the intrusive non-granitic related deposits were characterized by both positive Ce and negative Eu anomalies (Corcoran et al., 2019).

As the C1- Chondrite pattern remained similar for the samples, comparison of the plot of ∑REE vs $(\sum LREE/\sum HREE)_{CN}$ plot (Fig. 7) was done. The plot showed that the uranium ore samples are in distinct clusters for each mine and not overlapping each other. The distinct cluster provides evidence of the different ore samples.

3.3. Determination of statistical differences

The nonparametric Kruskal-wallis test resulted in $p < 0.05$ for all samples providing a very strong evidence to suggest difference between at least one pair of the mines. The significant difference was done with the pair wise comparison test.

For all the elements in the pair M1-M2, the *p value* is less than 0.05 suggesting a very strong evidence of the differences between the samples from M1 and M2. This suggested that M1 and M2 are from different geological deposit. There was no evidence of difference between the pair M1 – M3 as the *p value* was greater than 0.05 for all elements. The pair M3-M2 results are inconclusive as the LREE *p value* is less than 0.05 but the HREE the *p value* is greater than 0.05. The PCA plot of the REE concentration is shown in Fig. 8. The samples are evidently clustered according to mine and showed the REE concentration difference between the mines.

4. Conclusion

Rare earth elements of uranium ore deposit were determined using ICP-MS. The uranium ore samples from the 3 mines showed similar REE patterns with pronounced negative Eu anomaly and flat HREE. The pair wise comparison test strongly suggests a significant difference in the

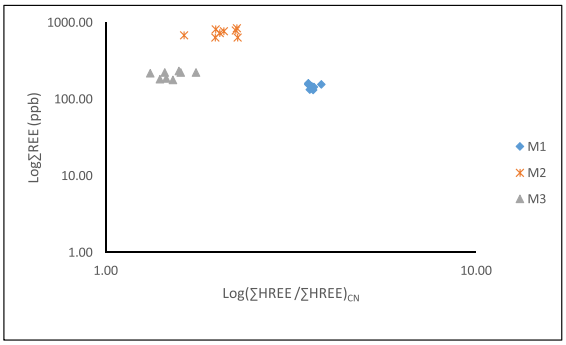

Fig. 7. ∑REE abundance versus sum of C1- chondrite light over heavy REE fractionation for uranium ore of M1, M2 and M3.

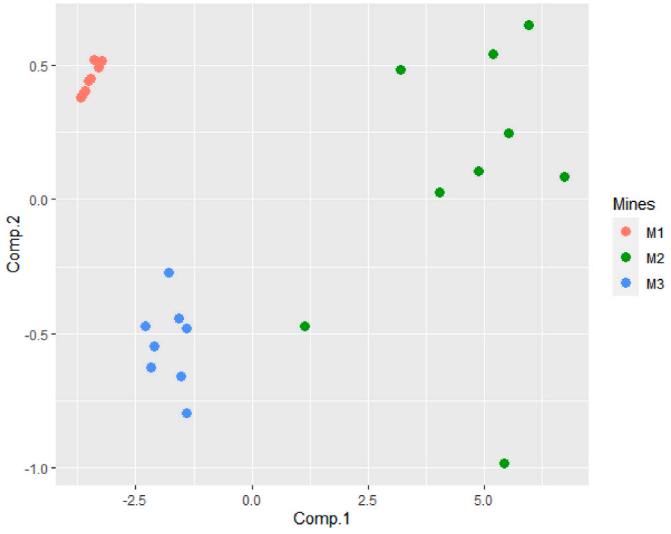

Fig. 8. PCA results of REE Concentrations from all uranium ore samples.

samples from M1 and M2 as the *p value* was less than 0.05 an indication that the samples deposits are different. The pair M1 and M3 *p value* was above 0.05 and suggest that there is no significant between the samples an indication that the samples deposit is similar.

The study has demonstrated that uranium ore deposits from the 3 mines in Namibia could be distinguished using their REE concentration and pattern.

The study suggests that the negative Eu anomaly, enriched LREE, depleted HREE and higher fractionation of LREE compared to HREE observed is a nuclear forensic signature for the Namibia uranium ore deposits.

It is recommended that comprehensive sampling be undertaken to give the full view of the REE nuclear forensics signatures at the different stage of the nuclear fuel cycle (cradle to grave and mining to waste characterization).

Declaration of competing interest

The authors declare that they have no known competing financial interests or personal relationships that could have appeared to influence the work reported in this paper.

Acknowledgement

The authors would like to acknowledge the Council for Scientific and Industrial Research (CSIR), Department of Science and Innovation (DSI)

inter-bursary and the Innternational Atomic Energy Agency, Vienna, Austria [research grant no. CRP2300] financial support for the project. Appreciation to the uranium mines for providing access to the mines for sample collection and the staff at Center of Applied Radiation Science and Technology (CARST) nuclear forensic laboratory for sample analysis.

References

Anders, E., Grevesse, N., 1989. Abundances of the elements: meteoritic and solar. Geochem. Cosmochim. Acta 53, 197–214.

Bahariya, G.A.E., 2018. Geochemistry and tectonic setting of neoproterozoic rocks from the arabian-nubian shield: emphasis on the Eastern Desert of Egypt. In: Applied Geochemistry with Case Studies on Geological Formations, Exploration Techniques and Environmental Issues. Intechopen.

Balboni, E., Simonetti, A., Spano, T., Cook, N.D., Burns, P.C., 2017. Rare-earth element fractionation in uranium ore and its U(VI) alteration minerals. Appl. Geochem. 87, 84–92.

Basson, I., Greenway, G., 2004. The rossing uranium deposit: a product of late- kinematic localization of uraniferous granite in the central- zone of the Damara Orogen, Namibia. J. Afr. Earth Sci. 38, 413–435.

Bazilio, A., Weinrich, J., 2012. The easy guide to: inductively coupled PlasmaMass spectrometry (ICP-MS) [Online]. Available: www.ecs.umass.edu/eve/facilities/equipment/ICPMS/ICPMS%20quick%20guide.pdf. (Accessed 9 January 2019).

Bradley, V.C., Manard, B.T., Roach, B.D., Metzger, S.C., Rogers, K.T., Ticknor, B.W., Wysor, S.K., Brockman, J.D., Hexel, C.R., 2020. Rare earth element determination in uranium ore concentrates using online and offline chromatography coupled to ICP-MS. Minerals 10.

Corcoran, L., Simonetti, A., Spano, T.L., Lewis, S.R., Dorais, C., Simonetti, S., Burns, P.C., 2019. Multivariate analysis based on geochemical, isotopic, and mineralogical compositions of uranium-rich samples. Minerals 9.

Donard, A., Pottin, A.-C., Pointurier, F., Pécheyran, C., 2015. Determination of relative rare earth element distributions in very small quantities of uranium ore concentrates using femtosecond UV laser ablation–SF-ICP-MS coupling. J. Anal. Atomic Spectrom. 30, 2420–2428.

Falster, A., Simmons, W., Webber, K., Boudreaux, A.P., 2018. Mineralogy and geochemistry of the Erongo sub-volcanic granitemiarolitic-pegmatite complex, Erongo, Namibia. Can. Mineral. 56, 425–449.

Frimmel, H.E., Schedel, S., Brätz, H., 2014. Uraninite chemistry as forensic tool for provenance analysis. Appl. Geochem. 48, 104–121.

Hutcheon, I., Kristo, M., Knight, K., 2015. Nonproliferation Nuclear Forensics.

IAEA, 2002. IAEA Safeguards Glossary. IAEA, Vienna.

IAEA, 2009. World Distribution of Uranium Deposits (UDEPO) with Uranium Deposit Classification. IAEA.

IAEA, 2015. Advances in nuclear forensics: countering the evolving threat of nuclear and other radioactive material out of regulatory control. Vienna, Austria.

IAEA, 2018a. Development of national nuclear forensic library: a system for the identification of nuclear or other radioactive material out of regulatory contrrol, Vienna, Austria.

IAEA, 2018b. World distribution of uranium deposits (UDEPO), TecDoc 1843. Vienna, Austria.

IAEA, 2020. Descriptive uranium deposit and mineral system models, Vienna, Austria.

Kanyan, N.K., 2015. Petrology and geochemistry of the granites and associated pegmatites in narnaul area district mahendragarh Haryana india petrogenesis and mineralization.

Keegan, E., Kristo, M.J., Colella, M., Robel, M., Williams, R., Lindvall, R., Eppich, G., Roberts, S., Borg, L., Gaffney, A., Plaue, J., Wong, H., Davis, J., Loi, E., Reinhard, M., Hutcheon, I., 2014. Nuclear forensic analysis of an unknown uranium ore concentrate sample seized in a criminal investigation in Australia. Forensic Sci. Int. 240, 111–121.

Keegan, E., Kristo, M.J., Toole, K., Kips, R., Young, E., 2016. Nuclear forensics: scientific analysis supporting law enforcement and nuclear security investigations. Anal. Chem. 88, 1496–1505.

Keegan, E., Richter, S., Kelly, I., Wong, H., Gadd, P., Kuehn, H., Alonso-Munoz, A., 2008. The provenance of Australian uranium ore concentrates by elemental and isotopic analysis. Appl. Geochem. 23, 765–777.

Khumalo, N., Mathuthu, M., 2018. Determination of trace elements and lanthanide (REE) signatures in uranium mine products in South Africa by means of inductively coupled plasma mass spectrometry. J. Geochem. Explor. 186, 235–242.

Lamount, S., Brisson, M., Curry, M., 2011. The USA national nuclear forensics library, nuclear materials information program, and data dictionary [Online]. Available: https://permalink.lanl.gov/object/tr?what=info:lanl-repo/lareport/LA-UR-11-00670 [Accessed 2020].

Mayer, K., Wallenius, M., Lützenkirchen, K., Galy, J., Varga, Z., Erdmann, N., Buda, R., Kratz, J., Trautmann, N., Fifield, K., 2011. Nuclear forensics: a methodology applicable to nuclear security and to non-proliferation. In: Journal of Physics: Conference Series. IOP Publishing, 062003.

Mercadier, J., Cuney, M., Lach, P., Boiron, M.-C., Bonhoure, J., Richard, A., Leisen, M., Kister, P., 2011. Origin of uranium deposits revealed by their rare earth element signature. Terra. Nova 23, 264–269.

Miller, R.M., 2008. The early neoproterozoic rocks. In: The Geology of Namibia. *Ministry of Mines and Energy*, vol. 2. Geological Survey of Namibia.

MME, 2010. Strategic Environmental Assessment for the Central Namib Uranium Rush. Ministry of Mine and Energy, Windhoek, Namibia.

MURD, 2020. Erongo region local authority [Online]. Available: http://www.murd.gov.na/erongo-local-authority. (Accessed 10 August 2020).

Ntsohi, L., Usman, I., Mavunda, R., Kureba, O., 2020. Characterization of uranium in soil samples from a prospective uranium mining in Serule, Botswana for nuclear forensic application. J. Radiat. Res. Appl. Sci. 1–11.

NUA, 2019. Uranium minning in Namibia [Online]. Available: www.namibianuranium.org. (Accessed 20 March 2019).

Perkinelmer, 2017. Titan MPS customer user guide [Online]. Available: http://www.perkinelmer.com.

Reading, D.G., 2016. Nuclear Forensics: Determining the Origin of Uranium Ores and Uranium Ore Concentrates via Radiological, Elemental and Isotopic Signatures. University of Southampton.

Reading, D.G., Croudace, I.W., Warwick, P.E., Cigliana, K.A., 2016. Applying multivariate statistics to discriminate uranium ore concentrate geolocations using (radio)chemical data in support of nuclear forensic investigations. J. Environ. Radioact. 162–163, 172–181.

Rosa, D.S., Sarkis, J.E., 2011. Rare Earths in Uranium Compounds and Important Evidences for Nuclear Forensic Purposes.

RSTUDIO TEAM, 2020. RStudio. Integrated Development for R. RStudio, PBC, Boston, MA [Online]. Available: http://www.rstudio.com/.

Spano, T.L., Simonetti, A., Balboni, E., Dorais, C., Burns, P.C., 2017. Trace element and U isotope analysis of uraninite and ore concentrate: applications for nuclear forensic investigations. Appl. Geochem. 84, 277–285.

Švedkauskaitė-Legore, J., Rasmussen, G., Abousahl, S., Van Belle, P., 2008. Investigation of the sample characteristics needed for the determination of the origin of uranium-bearing materials. J. Radioanal. Nucl. Chem. 278, 201–209.

Thomas, R., 2008. Practical Guide to ICP-MS: A Tutorial for Beginners. CRC Press, Boca Raton.

Toé, W., Vanderhaeghe, O., André-Mayer, A.S., Feybesse, J.L., Milési, J.P., 2013. From migmatites to granites in the Pan-African Damara orogenic belt, Namibia. J. Afr. Earth Sci. 85, 62–74.

Varga, Z., Wallenius, M., Mayer, K., 2010. Origin assessment of uranium ore concentrates based on their rare-earth elemental impurity pattern. Radiochim. Acta Int. J. Chem. Aspects Nucl. Sci. Technol. 98, 771–778.

Wang, L., Liang, T., 2015. Geochemical fractions of rare earth elements in soil around a mine tailing in Baotou, China. Sci. Rep. 5, 12483.

WNA, 2019. World uranium production [Online]. Available: http://www.world-nuclear.org/information-library/facts-and-figures/uranium-production-figures.aspx. (Accessed 20 March 2020).